

Three-stage carbon release model during macrophyte decomposition

Te Luo^{a,1}, Tingting Yang^{a,1}, Lu Wang^{a,1}, Ranran Wang^a, Yaqin Wang^a, Jing Yang^a, Zhou Tong^a, Feng Chen^b, Shanjun Wei^a, Pengfei Hei^{a,*}

^a College of Life and Environmental Science, Minzu University of China, Beijing 100081, China

^b Administration Bureau of Urat Wetland National Nature Reserve, Bayannur, Inner Mongolia 015000, China



ARTICLE INFO

Keywords:
 Carbon
 Nutrient release
 Model
 Macrophyte
 Decomposition
 Eutrophication
 Lake

ABSTRACT

Carbon release during macrophyte decomposing is critical for the carbon cycle in the aquatic ecosystems. Previous mechanistic researches have demonstrated the different release rates of nutrients in different stages, e.g., the fast-leaching stage (in initial 4–10 days), the microbe conditioning stage with slow decay rate (from winter to spring with low temperature). Nevertheless, models for predicting these processes are still not available and the conventional used model inherently assumes a constant relative release rate. Here, we conducted a one-year in-situ decomposition experiment using the conventional (net) litterbag technique. The credibility of experimental data is increased by using fresh debris to avoid alternation of material traits caused by the conventional drying pretreatment, which is originally used in experiments for terrestrial debris. Our results demonstrated that the carbon release process showed an obvious three-stage pattern, which can be universally depicted by a piecewise three-stage exponential decaying model ($r^2 > 0.9$). More importantly, contributions of the three key factor (i.e., leaching, microbe and macroinvertebrate) can be explicitly reflected by the corresponding relative release rate (k_i , i denote i th decomposition stage), which variate greatly between different stages, with $k_1/k_2 > 11.8$ and $k_3/k_2 > 2.63$. More importantly, k_3 can be further conveniently decomposed into microbe-induced k_{3-1} and macroinvertebrate-induced k_{3-2} , correspondingly. Also, k_{3-2} showed an exponential increase with the number of macroinvertebrate ($r^2 > 0.95$). The contributions of the microbe and macroinvertebrate can then be depicted by these two parameters. In conclusion, our model greatly increases the model realism and generality in simulating the carbon release process; Also, the explicit physical meaning of model parameters make the model mechanism clearer. This not only created the chance to further develop a mechanism-based model, but also facilitate the mechanistic study of the impacts of environmental factors (e.g., pH, dissolved oxygen) on k_1 , k_2 , k_{3-1} and k_{3-2} concerning different kinds of macrophyte, in which the parameters k_1 , k_2 , k_{3-1} and k_{3-2} acts as important ecological indicators in depicting the relative release rates caused by specific driving forces. These ecological indicators facilitate the future mechanical researches for the impacts of environmental factors on the carbon release.

1. Introduction

The carbon (C) cycle in ecosystems has received increased interest due to its impacts on the climate change (Bai and Cotrufo, 2022). In past decades, significant research has been conducted to investigate the C cycle in terrestrial ecosystems (e.g., forest, grassland and farmland) (Krishna and Mohan, 2017; Walker et al., 2018; Zeng et al., 2022; Bai and Cotrufo, 2022) and aquatic ecosystems (e.g., wetland, river, lake) (Xie et al., 2016; Xiao et al., 2017; Tang et al., 2018; Luo et al., 2020). During vegetation growth, large amounts of carbon are stored in the

vegetations (Yang et al., 2023; Qiu et al., 2020; Zhang et al., 2018; Zhang et al., 2021; Dai et al., 2020) and C gradually return to the soil or sediment pool during the deposition (Seastedt et al., 1992; Krishna and Mohan, 2017) or potentially release to the atmosphere (Zeng et al., 2022) as carbon source (Wohl et al., 2017). This process is especially prominent in wetlands and the macrophyte dominated eutrophication (MDE) lakes which are characterized by the overgrowth of tolerant macrophytes (Hei et al., 2019; Zhang et al., 2021; Wang et al., 2022).

Ecological models have been generally considered as an indispensable tool for supporting ecological decisions (Schmolke et al., 2010;

* Corresponding author.

E-mail addresses: heipf2010@muc.edu.cn, 2010042@muc.edu.cn (P. Hei).

¹ Co-first author.

Oberpriller et al., 2021). Unfortunately, detailed carbon release processes during macrophyte decomposition are generally not clear, and the early exponential decaying model (Olson, 1963) was commonly used to represent the nutrient release process (e.g., Xiao et al., 2017), which inherently assume a constant relative release rate throughout the decomposition. However, previous studies have indicated that nutrient release is rapid during the initial 4 days of macrophyte decomposition caused by rapid leaching of soluble material (Tukey, 1970; Fischer et al., 2006; Zhang et al., 2018; Luo et al., 2020), followed by a slower nutrient release stage dominated by microbial metabolism (Shilla et al., 2006; Han et al., 2019; Zhao et al., 2021). Also, previous researchers have documented that microbial metabolism could increase with the increase of the temperature (Godshalk and Wetzel, 1978; Migliorini and Romero, 2020; Zhao et al., 2021). Some research also mentioned the important impacts of the fragmentation of macroinvertebrates (e.g., Luo et al., 2020). All of these researches demonstrated that the relative release rate cannot be constant, hence the simple exponential model might be not suitable to be used in modelling the carbon release processes. Thus, more realistic models should be developed, but this could be achieved only when the more realistic experimental data is available.

Net litterbag (or litter bag) experiments are the most effective methods in the field decomposition experiment for macrophyte (Bocock and Gilbert, 1957; Wardle et al. 1997; Chen et al., 2021; Spohn and Berg, 2023). However, all the previous researches still used the drying pre-treatment (e.g., Carpenter and Adams, 1979; Dinka et al., 2004; Chimney and Pietro, 2006; Lan et al., 2006; Li et al., 2013; Carvalho et al., 2015; Wei et al., 2020), which is originally used in terrestrial vegetation decomposition researches. For aquatic vegetations, this drying pre-treatment inevitably decrease the credibility of experiments by introducing this additional drying and rehydration processes: Previous researches (e.g., Zhang et al., 2018) showed that the treatment of drying and rewetting cycles can accelerate the decomposition rate of leaf litter.

Here, the detailed carbon release processes of macrophytes were investigated by an in-situ experiment in sub-lakes of a typical MDE lake (Wuliangsu Lake, China) using the conventional litterbag methods. The credibility of the experimental data is increased by directly using the fresh debris. Based on these experimental data, we endeavor to establish a more realistic carbon release model considering the impacts of dominated driving forces in different release stages, which can greatly enhance the simulation ability for the carbon release processes.

2. Materials and methods

2.1. Site description

The field experiment was conducted in Wuliangsu Lake ($40^{\circ}36' - 41^{\circ}03'N$, $108^{\circ}43' - 108^{\circ}57'E$), the largest lake in the Yellow River Basin in China (366 km^2) (Fig. 1) (Yang et al., 2019; Zhang et al., 2021). This lake is primarily fed by irrigation water ($5.7 \times 10^8 \text{ m}^3$) from Hetao Irrigation regions. Eighty-one percent water was inflow through the Total Drainage Outlet ($4.6 \times 10^8 \text{ m}^3$) of drainage regions, and only 10 % water is discharged through the single lake outlet (located in the southernmost sub-lake as shown in Fig. 1) to the Yellow River (Yang et al., 2019). Wuliangsu Lake developed into a typical MDE lake after the 1990 s. *Phragmites australis* (emergent macrophyte) extends to 60 % of the area, and annual senescent biomass amounts to $1.0 \times 10^5 \text{ t}$ (dry mass, leaf/stem ratio is 1:6.5) (Hei et al., 2019), which divide the lake into 13 sub-lakes. These sub-lakes are primarily connected by narrow constructed net channels. Apart from the southernmost sub-lake, >90 % of the area in open sub-lakes are covered by dense *Potamogeton pectinatus* L. (submerged macrophyte). Among these sub-lakes, West sub-lake is most seriously affected by the inflow irrigation water, while East sub-lake, as nature reserve, is the least disturbed by human activity.

2.2. In-situ experiment

Senescent biomass of *P. australis* and *P. pectinatus* was collected prior to deposition on October 30, 2020 in Wuliangsu Lake. The biomass was washed free of sediment. *P. australis* detritus was separated into leaf and stem after collection. The *P. pectinatus* detritus was cut into two sizes (approximately 50 cm and 5 cm) after cleaned for convenience to assess the role of physical fragmentation. Each section was mixed thoroughly to ensure homogeneous content of moisture and total carbon (TC). The macrophyte detritus were placed in litter bags ($60 \text{ cm} \times 40 \text{ cm}$) with 30.0 g for *P. australis* leaf, 30.0 g for *P. australis* stem and 200.0 g *P. pectinatus*. Two mesh sizes (0.5 mm and 1.0 mm) were used to assess the potential role of invertebrates on debris breakdown as detailed by Graça (2001). Detailed experimental treatments are shown in Table 1. Replicate litter bags for each treatment were randomly selected for determining the initial drying mass and TC contents for *P. australis* stem, *P. australis* leaf and *P. pectinatus*. Totally 252 litter bags (14 treatments \times

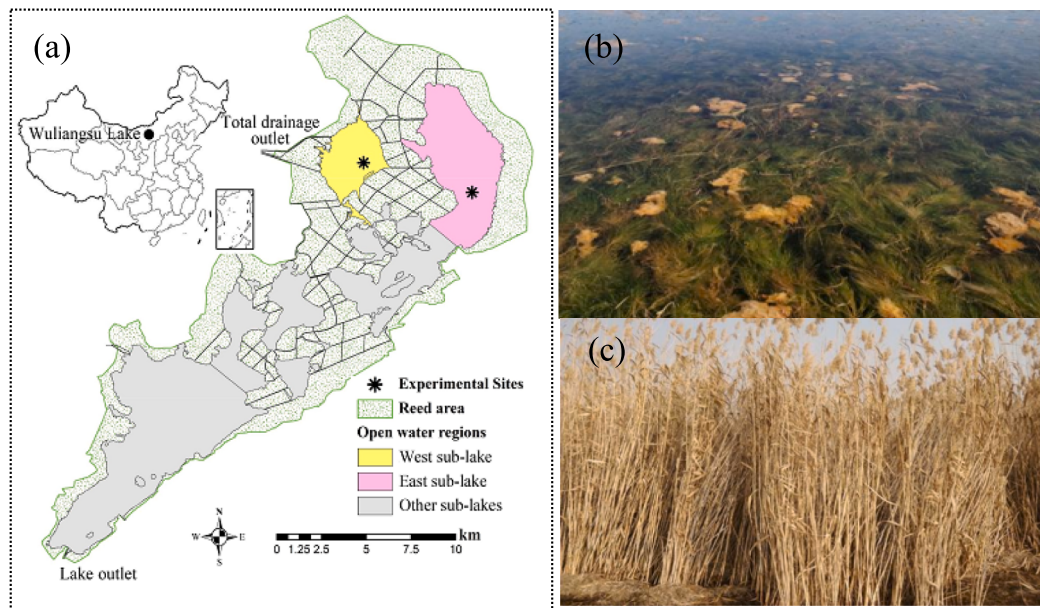


Fig. 1. The studying area in Wuliangsu lake:(a) experimental sites in two sub-lakes, (b) sub-lakes covered filled with *P. pectinatus* and (c) overgrown *P. australis* in reed area.

Table 1

Treatments of experiments for carbon release in debris decomposition processes. X denotes the sub-lake (X = W for West sub-lake and X = E for East sub-lake); Y denotes the vertical position of litter bags (Y = S for the sediment sample and Y = W for the water sample); M denotes the fragmentation size (5 or 30 cm) of *P. pectinatus* or the leaf, stem of *P. australis*; N denotes the mesh size of litter bags in the experiment. Water samples (W) were places at 0.5 m above the lake bottom.

Sub-lakes	Macrophyte detritus	Water depth	Fragmentation (cm)	Mesh size (mm)	Abbreviation X_Y_M–N
East sub-lake	<i>P. pectinatus</i>	Lake bottom	5	0.5, 1.0	E_S_5-0.5/1.0
			30	0.5, 1.0	E_S_30-0.5/1.0
	<i>P. australis</i>	Water	30	1.0	E_W_30-1.0
			/	1.0	E_W_Leaf-1.0
	<i>P. australis</i>	stem	40	1.0	E_W_Stem-1.0
			/	1.0	E_W_Water-1.0
	West sub-lake	Lake bottom	5	0.5, 1.0	W_S_5-0.5/1.0
			30	0.5, 1.0	W_S_30-0.5/1.0
		Water	30	1.0	W_W_30-1.0
			/	1.0	W_W_Leaf-1.0
		stem	40	1.0	W_W_Stem-1.0

9 retrieving times \times 2 duplication) were placed in two sub-lakes (shown in Fig. 1) on November 1, 2020.

The litter bags were sequentially retrieved after 4 d (Nov.5, 2020), 10 d (Nov.11, 2020), 70 d (Jan.1, 2021), 110 d (Feb.21, 2021), 160 d (Apr.11, 2021), 200 d (May.21, 2021), 240 d (Jul.1, 2021), 310 d (Sept.10, 2021), 365 d (Nov.1, 2021). At each sampling time, 28 litter bags were retrieved without disturbing the other bags, and then packed (4°C) and immediately transported to the laboratory within 24 h. The detritus in litter bags was firstly washed and the weight of the remaining dry mass is measured after the detritus was freeze-dried. Two grams of dried detritus was combusted at 525°C in a furnace for 4 h, and reweighed, and AFDM was then estimated by the mass loss during combusting. The concentration of TC was analyzed after the air-dried debris ground to fine powders (0.25 mm). The TC concentrations were analyzed by the elemental analyzer instrument (FLASH 2000, CHNS/O, Thermo Fisher Scientific Inc., UK).

2.3. Statistical analysis

The remaining ratio (RR) of carbon was used to denote the relative residual rate during debris decomposition.

$$RR = \frac{M_t C_t}{M_0 C_0} \times 100\% \quad (1)$$

where, M_t is the dry mass of detritus at time t (g), M_0 is the initial dry mass of debris at time 0 (g), C_t , C_0 is the TC concentration at day t and at day 0 (mg/g), respectively.

Paired samples t-test is used to study the significant difference between different treatments in Table 1. Nonlinear curve fitting is conducted using OriginPro 2019.

3. Results and discussion

3.1. Experimental data

3.1.1. AFDM loss ratio (%)

For *P. pectinatus*, AFDM loss processes can be generally divided into three stages (Fig. 2). AFDM losses in the 0–4 days amounted to almost $16.45 \pm 3.39\%$ in East sub-lake and $16.43 \pm 4.07\%$ in West sub-lakes, respectively. The decomposition rate becomes much smaller in the second stage, with total AFDM loss of $28.19 \pm 2.43\%$ (in East sub-lake) and $30.29 \pm 5.05\%$ (in West sub-lake) in the 4–200 days, respectively. During the period of previous two stages, AFDM loss ratio showed no significant difference between East sub-lake and West sub-lake. However, in the third stage, the AFDM loss in West sub-lake ($47.84 \pm 4.96\%$) was significantly higher than that in East sub-lake ($37.30 \pm 4.05\%$).

AFDM loss processes of *P. australis* leaf also showed a three-stage decomposition pattern. The first stage (0–4 d) was also characterized by rapid AFDM loss of 13.0–15.8 %, followed by a slow variation stage similar to *P. pectinatus*, with 26.7–28.3 % AFDM lost in the second stage (4–160 d). However, *P. australis* leaf stepped into the third stage early in 160 d, and AFDM loss accounted to almost 56.9–58.0 % in the third stage.

P. australis stem is resistant to the decomposition. The mass loss rate was much lower than that of *P. australis* leaf and *P. pectinatus*. Only approximate 58 % of the AFDM were lost during the studied period.

3.1.2. TC release

1) TC remaining ratio

TC remaining ratio showed a similar variation with AFDM remaining ratio for all treatments as shown in Fig. 3. For *P. pectinatus*, TC released rapidly in the initial short 0–4 days: the total release accounted for $16.77 \pm 3.10\%$ in East sub-lake and $15.14 \pm 4.36\%$ in West sub-lake, separately, although this release rate is still smaller than that of AFDM loss. The release rate became much slower in the second stage (4–200 d), with total release of $27.22 \pm 3.81\%$ in East sub-lake and $29.66 \pm 4.37\%$ in West sub-lake, respectively. Also, in these first two stages, there is no

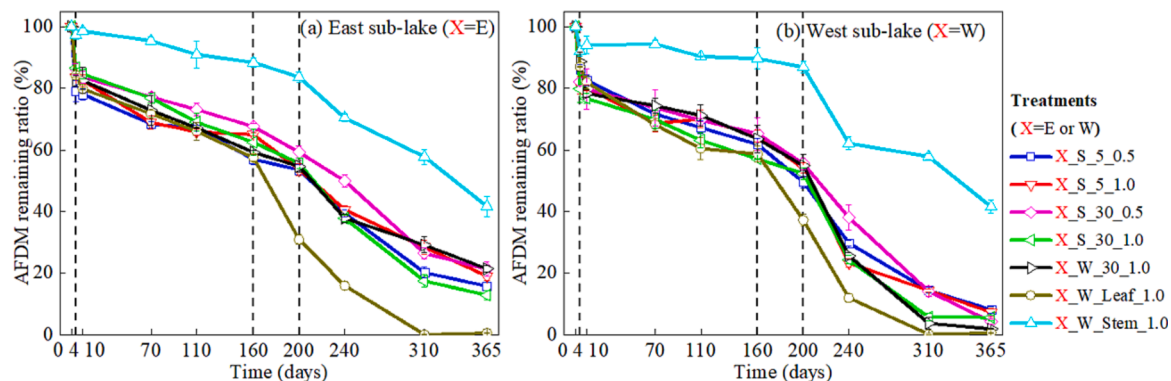


Fig. 2. Variation of AFDM remaining ratio during decomposition processes (see Table 1 for specific treatments X_Y_M–N). The error bar represents the standard error of the duplicated samples retrieved each time for each treatment.

significant difference between East sub-lake and West sub-lake. However, the release rates showed an obvious increase in the third stage, and TC release in West sub-lake ($48.97 \pm 4.71\%$) were significantly higher than that in East sub-lake ($34.84 \pm 4.72\%$).

For *P. australis* leaf, TC release rate showed similar variation with that of AFDM throughout the three stages. Also, little difference of TC release existed between East sub-lake (13.21 %, 26.38 % and 59.66 % in each stage, respectively) and West sub-lake (15.62 %, 26.05 %, 57.38 %, respectively). Only less than 1 % TC remains in the debris at the end of third stage. However, TC release from *P. australis* stem are significant slower, especially in the first stage, with only <1 % TC released in East sub-lakes. Also, almost 55 % TC remains in the macrophyte debris at the end of third stage.

2) TC contents

As shown in Fig. 4, TC contents did not exhibit similar variation with the biomass loss. In the initial 0–4 days, TN contents in *P. pectinatus* exhibits an obvious increase of 20.93–41.26 mg/g (in East sub-lake) and of 23.28–43.07 mg/g (in West sub-lake), separately. *P. australis* leaf also exhibits similar variation trends, with 20.93–41.26 mg/g and 23.28–43.07 mg/g increase in East and West sub-lake, separately. But the TC contents increase in *P. australis* stem was small (<4 mg/g). In the second stage, TC contents for all treatments showed a small decrease of 7.66–41.82 mg/g (in East sub-lake) and 19.94–52.73 mg/g (in West sub-lake). TC contents decreased again in the third stage (160 d for leaf, and 200 d for others). During all these stages, large increase in contents more likely occurred when there was the large mass loss for all treatments.

3.1.3. Eco-environment conditions

The water temperature in each time is shown in Table 2. We can see that water temperature was >20 °C during 200–310 d. It should be also noted that, during this time, large numbers of macroinvertebrates were found in the litter bags. Number of macroinvertebrates in West sub-lake ($x_{n,W}$) was generally larger than that in East sub-lake ($x_{n,E}$), with $x_{n,W}/x_{n,E}$ of 11.47 ± 6.62 .

3.2. Three-stage release model

Our results indicated that, during the initial several days, rapid loss occurred for both debris mass and TC, followed by comparatively slower variation in second stages, and then the loss rate is increased again in the third stage until reaching equilibrium. Thus, we propose a piecewise function using universal exponential decline formula,

$$W = \begin{cases} W_{10}e^{-k_1 t}, & 0 \leq t < t_1 \\ W_{20}e^{-k_2(t-t_{20})}, & t_1 \leq t < t_2 \\ W_{30}e^{-k_3(t-t_{30})}, & t_2 \leq t < t_3 \end{cases} \quad (2)$$

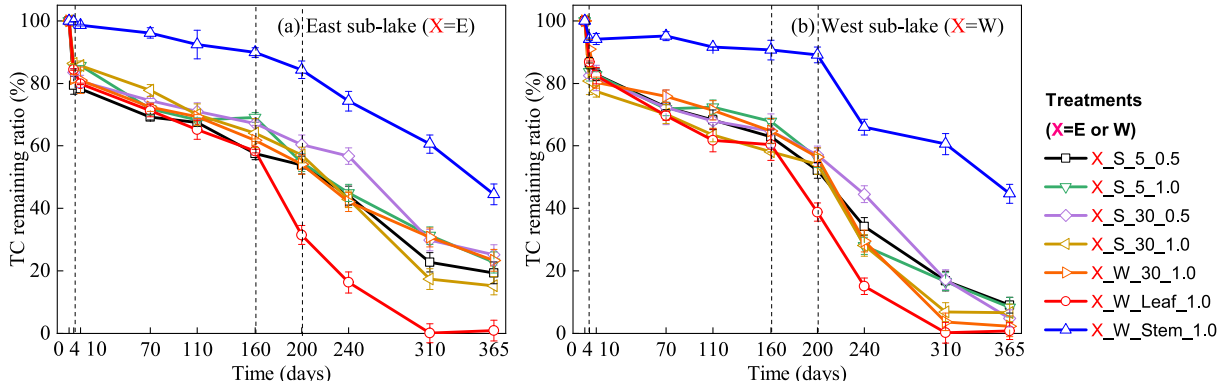


Fig. 3. Variation of TC remaining ratio during decomposition processes for different treatments (see Table 1 for specific treatments X_Y_M–N). The error bar represents the standard error of the duplicated samples retrieved each time for each treatment.

where, t is the time (d); t_i is end time of i th stage ($i = 1, 2, 3$); k_i ($i = 1, 2, 3$) is the decomposition rate coefficient (d^{-1}) of i th stage, respectively; W_{i0} ($i = 1, 2, 3$) are the initial remaining ratio in i th stage.

It can be seen from Fig. 6 and Table 3 that, for all treatments, $r^2 > 0.95$ with one exception for *P. australis* stem (in West sub-lake). Our piecewise function can clearly depict the AFDM loss and TC release processes in all three stages.

3.3. Contributions of key factors for k_i and modeling

1) Correlation of AFDM loss and TC release

Correlation analysis of parameters (w_i and k_i) in Eq. (2) between TC and AFDM indicated a high correlation between TC release and AFDM loss, with $r^2 > 0.96$ in first two stages and $r^2 > 0.99$ in third stages. From this we can infer that TC loss mainly caused by the debris decay. But TC contents showed an increase both in the first and in the third stage, which coincide with large mass loss periods. This means that TC loss rate is slower than AFDM loss rates. Also, in the third stage, the water temperature increased up to 20 °C, which is favored for the growth of microbe and microbial C might also contribute to an important part of the TC contents increase (Carvalho et al., 2005; Zhu et al., 2022).

2) Contributions of key factors for k_i

Further analysis of k_i in Table 3 indicated that 1) $k_1 > k_3 > k_2$, with $k_1/k_2 > 11.8$ and $k_3/k_2 > 2.63$ for all treatments except for *P. australis* stem; 2) no significance difference for k_1 , k_2 exists between East and West sub-lake; but 3) there is significant difference for k_3 between East and West sub-lakes for submerged macrophyte, with $k_{3,W}/k_{3,E} > 1.41$. Also, it should be noted that no significant difference was observed between treatments for fragmentation size (5 and 50 cm) and mesh size (0.5 and 1.0 mm). For the three stages, the variation pattern in first two stage can be well explained by the previous literatures: the first stage dominated by rapid leaching of soluble material (Fischer et al., 2006; Zhang et al., 2018; Luo et al., 2020) and the second stage is mainly dominated by microbial metabolism (Han et al., 2019). However, the third stage with a rebounded k_3 was seldom mentioned. Previous researchers have documented the important impacts of temperature on the microbial metabolism (Godshalk and Wetzel, 1978; Migliorini and Romero, 2020; Zhao et al., 2021). However, this thermal impact cannot explain the significant difference of k_3 between East and West sub-lakes because no difference of temperature exists between these two sub-lakes. Fortunately, this difference become explainable when the significant difference of macroinvertebrate between the two sub-lakes was considered; During the third stage, the number of macroinvertebrates in West sub-lake were 3.7 ~ 21 times of that in East sub-lake for all

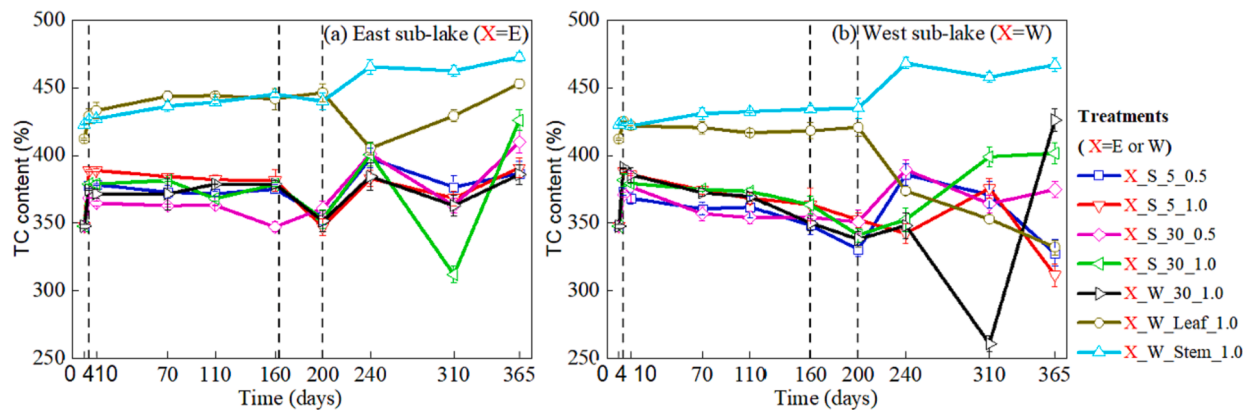


Fig. 4. Variation of TC contents in the debris for different treatment (see Table 1 for specific treatments X_Y_M–N). The error bar represents the standard error of the duplicated samples retrieved each time for each treatment.

Table 2
Water temperature (°C) at a depth of 0.5 m under the water surface.

Sampling Times	1	2	3	4	5	6	7	8	9	10
Days	0	4	10	70	110	160	200	240	310	365
Water temperature	7.7	5.4	5.7	0.6	3.1	14.2	23.9	26.1	22.7	8.6

treatments. More importantly, it offers us the opportunity for modeling the contributions of the macroinvertebrates based on the response of TC release rate to the macroinvertebrate number in different litter bags for *P. pectinatus*. Here, *P. australis* samples were not considered because the mass loss in *P. australis* samples is not sensitive to the macroinvertebrate numbers, with much smaller difference of k_3 between the two sub-lakes.

3) Modeling for k_3

Non-linear analysis showed that k_3-k_2 follows an exponential increase with macroinvertebrate number (x_N) for *P. pectinatus* samples:

$$k_3 - k_2 = ae^{bx_N} \quad (3)$$

where b is the relative increase rate of k_3-k_2 with x_N , and a is equal to k_3-k_2 when no macroinvertebrate participates ($x_N = 0$). The coefficients of Eq. (3) for both TC and AFDM were shown in Table 4.

Thus, k_3 can be further decomposed into two parts: microbe dominated rate (k_{3-1}) and macroinvertebrate dominated rate (k_{3-2})

$$k_3 = k_{3-1} + k_{3-2} \quad (4)$$

with

$$k_{3-1} = a + k_2 \quad (5)$$

$$k_{3-2} = k_3 - k_{3-1} = a(e^{bx_N} - 1) \quad (6)$$

Alternatively, if k_3 is known based on measured data in practice, k_{3-1} can also be attained based on k_3 and k_{3-2} , namely,

$$k'_{3-1} = k_3 - k_{3-2} \quad (7)$$

4) Variation of k_{3-1} and k_{3-2} in third stage

Fig. 7. showed k_{3-1} and k_{3-2} computed using Eqs. (5) and (6) based on parameter values of a , b in Table 4 and x_N in Fig. 5. We can clearly see the comparative contribution between microbe and macroinvertebrate on the mass loss rate k_3 . In East sub-lake with $x_N < 10$, macrophyte decomposition are generally dominated, with $k_{3-1}/k_3 > 95\%$. As the increase of x_N , k_{3-2} is increased obviously but k_{3-1} remains with little variation. It can be noticed that k_{3-2} supersedes k_{3-1} when x_N increases from

82 to 118.

More importantly, the TC remaining ratio in third stage can be predicted using Eq. (2) once the k_{3-1} and k_{3-2} is determined, in which k_{3-2} can be calculated based on the macroinvertebrate number (x_N).

3.4. Merits and limitations

3.4.1. Merits

1) Improvements in realism and accuracy of our model

Until now, almost all previous literatures (e.g., Zhang et al., 2008; Han et al., 2019; Vitale et al., 2019; Song and Jiang, 2020; Pan et al., 2021) directly used Olson's single exposure model (Olson, 1963) to model the nutrient release processes. Although our results fall in line with the previous literature in that carbon release processes show a similar variation pattern with the decomposition processes, our results

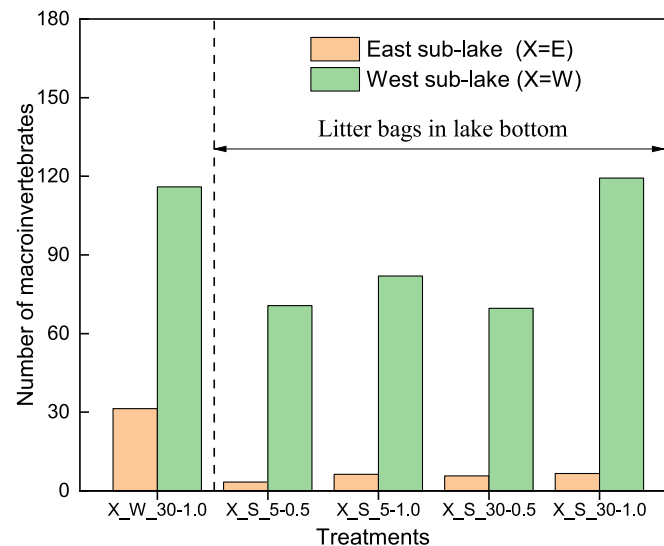


Fig. 5. Number of macroinvertebrates (Fruticicolidae) in retrieved samples for different treatments (see Table 1 for specific treatments X_Y_M–N).

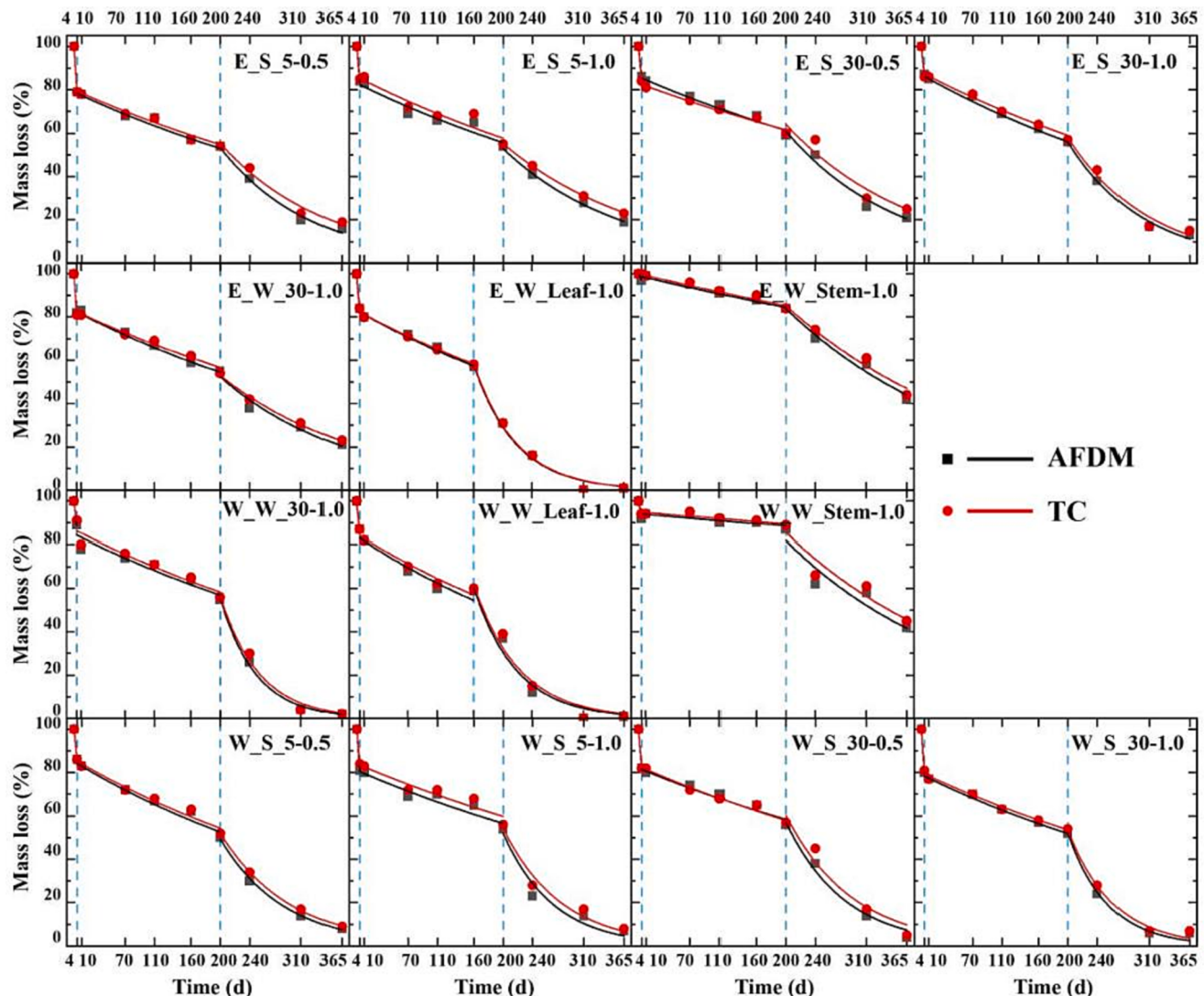


Fig. 6. Piecewise function model for AFDM loss and TC release (see Table 1 for specific treatments). All model parameters and coefficient of determination (r^2) are summarized in Table 3.

demonstrate a three-stage decomposition pattern: discrepancy of the relative decomposition rate between different stages amounts to 2–11 folds. This discrepancy certainly cannot be modeled by Olson's single exposure model which inherently assumes constant relative decomposition rate, but can be well modeled by a three-stage exponential model as detailed in Section 3.2. Also, prediction of the impacts of invertebrates on the decomposition rate becomes possible: if the number of invertebrates (x_N) is known, the relative decomposition rate k_{3-2} can be calculated based on the Eq. (6).

2) Transition towards mechanistic model

Mechanistic effect models have long been identified as potentially useful tools to extrapolate the limited findings from standard tests to more realistic conditions (Forbes et al., 2010; Thorbek et al., 2010). However, unlike physics models, most of the ecological model are empirical models and the mechanism is generically unclear due to lack of knowledge for mechanism, resources of money or time. When the model is applied to the working conditions with different driving factors or different scale, they might lead to erroneous decisions (Augusiaik et al., 2014). The single exponential model assumes a constant relative release rate at different stages, which could not reflect different driving factors, so the model completely lost the mechanism attribute. In our

three-stage model, the relative decomposition rate of different stages can reflect the impacts of different dominant driving factors. Even in the complex third stage, the key drive forces of both microorganisms and macroinvertebrate are successfully to be modeled by Eqs. (5)–(7). This increases the capacity of our model to reproduce observations for the right reasons, not just to tweak the parameters via calibration to do the right thing.

3) Potential use of our models

The model can be applied in two aspects. Firstly, the model can be used to predict the carbon release during the macrophyte decomposition after the model parameters are calibrated with measured data under similar conditions; Secondly, the models k_1 , k_2 , k_{3-1} and k_{3-2} can be used as important ecological indicators to characterize the carbon release rate driven by factors of leaching, microbes and macroinvertebrates. This facilitates further mechanical researches.

3.4.2. Limitations and challenges

Models are simplified representations of real systems (Augusiaik et al., 2014). Despite of large progresses in both model realism and mechanism for our model, the limitations still cannot be ignored.

Firstly, the model realism still restricted by the data realism. The data

Table 3

Fitting parameter for three-stage decomposition models (Eq. (2)) for (a) AFDM and (b) TC.

(a) AFDM treatment	k_1	r^2	W_{20}	k_2	r^2	W_{30}	k_3	r^2
E_S_5-0.5	0.0588	1.00	0.79	0.0020	0.98	0.54	0.0081	0.99
E_S_5-1.0	0.0450	1.00	0.83	0.0020	0.92	0.53	0.0061	0.99
E_S_30-0.5	0.0371	1.00	0.86	0.0017	0.97	0.61	0.0066	0.97
E_S_30-1.0	0.0359	1.00	0.87	0.0022	0.99	0.56	0.0097	0.99
E_W_30-1.0	0.0486	1.00	0.83	0.0021	1.00	0.52	0.0057	0.95
E_W_Leaf-1.0	0.0431	1.00	0.83	0.0023	0.98	0.58	0.0172	0.99
E_W_Stem-1.0	0.0070	1.00	0.99	0.0008	0.95	0.84	0.0039	0.97
W_S_5-0.5	0.0372	1.00	0.85	0.0024	0.96	0.49	0.0114	1.00
W_S_5-1.0	0.0527	1.00	0.81	0.0018	0.90	0.52	0.0146	0.93
W_S_30-0.5	0.0492	1.00	0.82	0.0017	0.95	0.57	0.0124	0.98
W_S_30-1.0	0.0563	1.00	0.79	0.0021	0.99	0.52	0.0185	0.99
W_W_30-1.0	0.0300	1.00	0.85	0.0020	0.89	0.55	0.0205	1.00
W_W_Leaf-1.0	0.0348	1.00	0.84	0.0027	0.93	0.61	0.0171	0.96
W_W_Stem-1.0	0.0209	1.00	0.94	0.0003	0.64	0.83	0.0041	0.85
(b) TC								
treatment	k_1	r^2	W_{20}	k_2	r^2	W_{30}	k_3	r^2
E_S_5-0.5	0.0577	1.00	0.79	0.0019	0.98	0.55	0.0068	0.97
E_S_5-1.0	0.0394	1.00	0.85	0.0020	0.89	0.55	0.0052	1.00
E_S_30-0.5	0.0450	1.00	0.83	0.0015	0.98	0.63	0.0057	0.90
E_S_30-1.0	0.0368	1.00	0.87	0.0020	0.99	0.58	0.0091	0.97
E_W_30-1.0	0.0512	1.00	0.82	0.0019	0.97	0.53	0.0051	0.99
E_W_Leaf-1.0	0.0425	1.00	0.83	0.0022	0.98	0.59	0.0171	0.99
E_W_Stem-1.0	0.0008	1.00	1.00	0.0008	0.95	0.85	0.0036	0.97
W_S_5-0.5	0.0364	1.00	0.85	0.0023	0.97	0.52	0.0105	1.00
W_S_5-1.0	0.0444	1.00	0.84	0.0017	0.90	0.54	0.0126	0.96
W_S_30-0.5	0.0484	1.00	0.82	0.0018	0.98	0.60	0.0110	0.94
W_S_30-1.0	0.0534	1.00	0.80	0.0020	0.99	0.54	0.0165	0.99
W_W_30-1.0	0.0238	1.00	0.87	0.0020	0.91	0.57	0.0189	0.98
W_W_Leaf-1.0	0.0354	1.00	0.84	0.0025	0.93	0.62	0.0162	0.96
W_W_Stem-1.0	0.0150	1.00	0.95	0.0003	0.76	0.85	0.0038	0.87

Table 4

Fitting parameter Eq. (3).

a	b	r^2	Freedom number
TC	0.00462 ± 0.00055	0.00951 ± 0.00132	0.93 7
AFDM	0.0450	1.00	0.91 7

credibility has been greatly increased by using the fresh debris without the conventional drying pretreatment in our experiments. However, all debris used in the experiments is harvested before placed in the net

litterbag, which is not the case in nature decomposition. This harvest treatment will certainly introduce some deviation for the carbon release processes, especially for the leaching processes. However, this limitation is seldom stressed and has not been solved in our work.

Secondly, although all parameters of k_1 , k_2 , k_{3-1} and k_{3-2} have explicit physical meaning, the response of the value of these parameters to the environmental factor (e.g., pH, dissolved oxygen, temperature, etc.) is still not clear. Thus, this model still needs to be calibrated for the parameters before used in predictions, and the calibrated parameters is practical only in specific regions with similar environmental conditions.

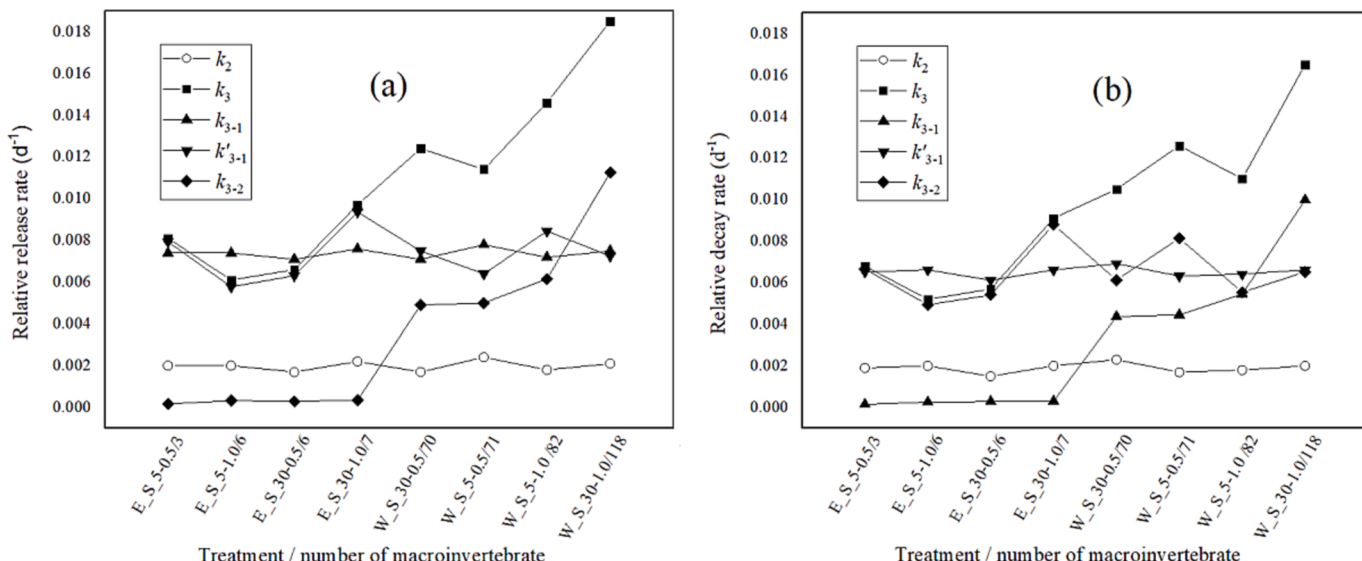


Fig. 7. Comparative contribution of microbe and macroinvertebrate on relative decay rate k_3 . k_3 is decomposed into two parts: the microbe dominated k_{3-1} and the macroinvertebrate dominated k_{3-2} . The x-axis also shows the corresponding treatment in which the number of macrophyte is observed as shown in Fig. 5. a) for TC and b) for AFDM.

4. Conclusions

In our work, we have developed a three-stage carbon release model, which is capable to depict the variation of carbon release processes in different stage during macrophyte decomposition. Model accuracy increased greatly, and the mechanism become clearer, but limitations still exist. In the near future, it is crucial to conduct experiments to investigate the mechanistic impacts of environmental factors on k_1 , k_2 , k_{3-1} and k_{3-2} , which act as important ecological indicators for the relative carbon release rate caused by different driving forces, and thereafter further increase the model accuracy and generality. This work seems huge and tedious, but the stake is high in developing a high mechanic model.

6. Authors' contribution

Pengfei Hei, Lu Wang and Te Luo conceived and designed the study. Te Luo, Lu Wang, Shanjun Wei and Jing Yang collected field data. Te Luo, Tong Zhou, Ranran Wang, and Yaqin Wang analyzed the samples. Te Luo, Lu Wang performed data and statistical analyses. Pengfei Hei, Te Luo and Lu Wang develop the models. Te Luo, Tingting Yang, Lu Wang wrote the manuscript. Pengfei Hei and Chen Feng revised the manuscript. All authors edited the manuscript and approved the final version of the manuscript.

Declaration of Competing Interest

The authors declare that they have no known competing financial interests or personal relationships that could have appeared to influence the work reported in this paper.

Data availability

Data will be made available on request.

Acknowledgements

We are grateful for the financial supports from the National Natural Science Foundation of China, China (grant numbers 51209239 and 51979297) and the Open Research Fund Program of the State Key Laboratory of Hydroscience and Engineering, China (grant number sklhse-2020-B-06).

References

- Augusiak, J., Van den Brink, P.J., Grimm, V., 2014. Merging validation and evaluation of ecological models to 'evaluation': A review of terminology and a practical approach. *Ecol. Model.* 280, 117–128.
- Bai, Y., Cotrufo, M.F., 2022. Grassland soil carbon sequestration: Current understanding, challenges, and solutions. *Science* 377 (6606), 603–608.
- Bocock, K.L., Gilbert, O.J.W., 1957. The disappearance of leaf litter under different woodland conditions. *Plant Soil* 9 (2), 179–185.
- Carpenter, S.R., Adams, M.S., 1979. Effects of nutrients and temperature on decomposition of *Myriophyllum spicatum* L. in a hard-water eutrophic lake 1. *Limnol. Oceanogr.* 24 (3), 520–528.
- Carvalho, C., Hepp, L.U., Palma-Silva, C., Albertoni, E.F., 2015. Decomposition of macrophytes in a shallow subtropical lake. *Limnologica* 53, 1–9.
- Carvalho, P., Thomaz, S.M., Bini, L.M., 2005. Effects of temperature on decomposition of a potential nuisance species: the submerged aquatic macrophyte *Egeria najas* planchonii (Hydrocharitaceae). *Braz. J. Biol.* 65 (1), 51–60.
- Chen, G.-T., Chen, Y.-Q., Peng, Y., Hu, H.-L., Xie, J.-L., Chen, G., Xiao, Y.-L., Liu, L.i., Tang, Y.i., Tu, L.-H., 2021. Standard litterbags underestimate early-stage lower-order root decomposition rate in a subtropical forest, China. *Plant Soil* 469 (1–2), 335–346.
- Chimney, M.J., Pietro, K.C., 2006. Decomposition of macrophyte litter in a subtropical constructed wetland in south Florida (USA). *Ecol. Eng.* 27 (4), 301–321.
- Dai, X., Yang, G., Liu, D., Wan, R., 2020. Vegetation Carbon Sequestration Mapping in Herbaceous Wetlands by Using a MODIS EVI Time-Series Data Set: A Case in Poyang Lake Wetland, China. *Remote Sens.* 12, 3000.
- Dinka, M., Ágoston-Szabó, E., Tóth, I., 2004. Changes in nutrient and fibre content of decomposing *Phragmites australis* litter. *Int. Rev. Hydrobiol.* 89 (5–6), 519–535.
- Fischer, H., Mille-Lindblom, C., Zwirnmann, E., Tranvik, L.J., 2006. Contribution of fungi and bacteria to the formation of dissolved organic carbon from decaying common reed (*Phragmites australis*). *Arch. Hydrobiol.* 166 (1), 79–97.
- Forbes, V.E., Calow, P., Grimm, V., Hayashi, T., Jager, T., Palmqvist, A., Pastorok, R., Salvito, D., Sibly, R., Spromberg, J., Stark, J., Stillman, R.A., 2010. Integrating population modeling into ecological risk assessment. *Inegr. Environ. Asses.* 6: 191193.
- Godshalk, G.L., Wetzel, R.G., 1978. Decomposition of aquatic angiosperms. II. Particulate components. *Aquatic Bot.* 5, 301–327.
- Graça, M.A.S., 2001. The role of invertebrates on leaf litter decomposition in streams—a review. *Int. Rev. Hydrobiol.* 86 (4–5), 383–393.
- Han, B., Addo, F.G., Mu, X., Zhang, L., Zhang, S., Lv, X., Li, X., Wang, P., Wang, C., 2019. Epiphytic bacterial community shift drives the nutrient cycle during *Potamogeton malaianus* decomposition. *Chemosphere* 236, 124253.
- Hei, P., Yang, T., Song, J., Zhang, J., Liu, W., Zhou, G., Yang, J., Liu, C., 2019. Integration of cleaner production (CP) and sustainable supply chain management (SSCM): CP+SSCM→CPSSCM-Inspired from impacts of Cleaner production on China's macrophyte-dominated eutrophic lakes. *J. Clean. Prod.* 234, 1446–1458.
- Krishna, M.P., Mohan, M., 2017. Litter decomposition in forest ecosystems: a review. *Energ. Ecol. Environ.* 2 (4), 236–249.
- Lan, N.K., Asaeda, T., Manatunge, J., 2006. Decomposition of aboveground and belowground organs of wild rice (*Zizania latifolia*): mass loss and nutrient changes. *Aquat. Ecol.* 40 (1), 13–21.
- Li, X., Cui, B., Yang, Q., Lan, Y., Wang, T., Han, Z., 2013. Effects of plant species on macrophyte decomposition under three nutrient conditions in a eutrophic shallow lake, North China. *Ecol. Model.* 252, 121–128.
- Luo, P., Tong, X., Liu, F., Huang, M., Xu, J., Xiao, R., Wu, J., 2020. Nutrients release and greenhouse gas emission during decomposition of *Myriophyllum aquaticum* in a sediment-water system. *Environ. Pollut.* 260, 114015.
- Migliorini, G.H., Romero, G.Q., 2020. Warming and leaf litter functional diversity, not litter quality, drive decomposition in a freshwater ecosystem. *Sci. Rep.* 10, 1–11.
- Oberpriller, J., Cameron, D.R., Dietze, M.C., Hartig, F., Coulson, T., 2021. Towards robust statistical inference for complex computer models. *Ecol. Lett.* 24 (6), 1251–1261.
- Olson, J.S., 1963. Energy storage and the balance of producers and decomposers in ecological systems. *Ecology* 44, 322–331.
- Pan, M., Wang, T., Hu, B., Shi, P., Xu, J., Zhang, M., 2021. Mesocosm Experiments Reveal Global Warming Accelerates Macrophytes Litter Decomposition and Alters Decomposition-Related Bacteria Community Structure. *Water*. 13, 1940.
- Qiu, Z., Feng, Z., Song, Y., Li, M., Zhang, P., 2020. Carbon sequestration potential of forest vegetation in China from 2003 to 2050: Predicting forest vegetation growth based on climate and the environment. *J. Clean. Prod.* 252, 119715.
- Schmolke, A., Thorbek, P., DeAngelis, D.L., Grimm, V., 2010. Ecological models supporting environmental decision making: a strategy for the future. *Trends Ecol. Evol.* 25 (8), 479–486.
- Seastedt, T.R., Parton, W.J., Ojima, D.S., 1992. Mass loss and nitrogen dynamics of decaying litter of grasslands: the apparent low nitrogen immobilization potential of root detritus. *Can. J. Bot.* 70 (2), 384–391.
- Shilla, D., Asaeda, T., Fujino, T., Sanderson, B., 2006. Decomposition of dominant submerged macrophytes: implications for nutrient release in Myall Lake, NSW, Australia. *Wet. Ecol. Manag.* 14 (5), 427–433.
- Song, N., Jiang, H., 2020. Coordinated photodegradation and biodegradation of organic matter from macrophyte litter in shallow lake water: dual role of solar irradiation. *Water Res.* 172, 11551.
- Spoehn, M., Berg, B., 2023. Import and release of nutrients during the first five years of plant litter decomposition. *Soil Biol. Biochem.* 176, 108878.
- Tang, W., Zheng, M., Zhao, X., Shi, J., Yang, J., Trettin, C.C., 2018. Big geospatial data analytics for global mangrove biomass and carbon estimation. *Sustainability* 10, 472.
- Thorbek, P., Forbes, V.E., Heimbach, F., Hommen, U., Thulke, H.-H., Van den Brink, P.J., Wogram, J., Grimm, V. (Eds.), 2010. Ecological Models for Regulatory Risk Assessments of Pesticides: Developing a Strategy for the Future. Society of Environmental Toxicology and Chemistry (SETAC) and CRC Press, *Pensacola and Boca Raton*, FL, USA.
- Tukey Jr, H., 1970. The leaching of substances from plants. *Annu. Rev. Plant Physiol.* 21, 305–324.
- Vitale, M., Amitrano, W., Hoshika, Y., Paoletti, E., 2019. Plant species-specific litter decomposition rates are directly affected by tropospheric ozone: Analysis of trends and modelling. *Water Air Soil Pollut.* 230, 1–22.
- Walker, T.W., Kaiser, C., Strasser, F., Herbold, C.W., Leblans, N.I., Woebken, D., Janssens, I.A., Sigurdsson, B.D., Richter, A., 2018. Microbial temperature sensitivity and biomass change explain soil carbon loss with warming. *Nat. Clim. Chang.* 8, 885–889.
- Wang, L., Yang, T., Hei, P., Zhang, J., Yang, J., Luo, T., Zhou, G., Liu, C., Wang, R., Chen, F., 2022. Internal phosphorus cycling in macrophyte-dominated eutrophic lakes and its implications. *J. Environ. Manag.* 306, 114424.
- Wardle, D., Bonner, K., Nicholson, K., 1997. Biodiversity and plant litter: experimental evidence which does not support the view that enhanced species richness improves ecosystem function. *Oikos* 247–258.
- Wei, Y., Zhang, M., Cui, L., Pan, X., Liu, W., Li, W., Lei, Y., 2020. Winter decomposition of emergent macrophytes affects water quality under ice in a temperate shallow lake. *Water*. 12, 2640.
- Wohl, E., Hall Jr, R.O., Lininger, K.B., Sutfin, N.A., Walters, D.M., 2017. Carbon dynamics of river corridors and the effects of human alterations. *Ecol. Monogr.* 87, 379–409.

- Xiao, L., Zhu, B., Kumwimba, M.N., Jiang, S., 2017. Plant soaking decomposition as well as nitrogen and phosphorous release in the water-level fluctuation zone of the Three Gorges Reservoir. *Sci. Total Environ.* 592, 527–534.
- Xie, Y., Xie, Y., Hu, C., Chen, X., Li, F., 2016. Interaction between litter quality and simulated water depth on decomposition of two emergent macrophytes. *J. Limnol.* 75 (1).
- Yang, T., Hei, P., Song, J., Zhang, J., Zhu, Z., Zhang, Y., Yang, J., Liu, C., Jin, J., Quan, J., 2019. Nitrogen variations during the ice-on season in the eutrophic lakes. *Environ. Pollut.* 247, 1089–1099.
- Yang, L., Lin, Y., Kong, J., Yu, Y., He, Q., Su, Y., Li, J., Qiu, Q., 2023. Effects of fertilization and dry-season irrigation on the timber production and carbon storage in subtropical Eucalyptus plantations. *Ind. Crop Prod.* 192, 116143.
- Zeng, X.-M., Feng, J., Yu, D.-L., Wen, S.-H., Zhang, Q., Huang, Q., Delgado-Baquerizo, M., Liu, Y.-R., 2022. Local temperature increases reduce soil microbial residues and carbon stocks. *Glob. Chang. Biol.* 28, 21.
- Zhang, J., Hei, P., Shang, Y., Yang, J., Wang, L., Yang, T., Zhou, G., Chen, F., 2021. Internal Nitrogen Cycle in Macrophyte-Dominated Eutrophic Lakes: Mechanisms and Implications for Ecological Restoration. *ACS. ES&T. Water.* 1, 2359–2369.
- Zhang, D., Hui, D., Luo, Y., Zhou, G., 2008. Rates of litter decomposition in terrestrial ecosystems: global patterns and controlling factors. *J. Plant Ecol.* 1, 85–93.
- Zhang, L., Zhang, S., Lv, X., Qiu, Z., Zhang, Z., Yan, L., 2018. Dissolved organic matter release in overlying water and bacterial community shifts in biofilm during the decomposition of *Myriophyllum verticillatum*. *Sci. Total. Environ.* 633, 929–937.
- Zhao, B., Xing, P., Wu, Q., L., 2021. Interactions between bacteria and fungi in macrophyte leaf litter decomposition. *Environ. Microbiol.* 23, 1130–1144.
- Zhu, L., Deng, Z., Xie, Y., Zhang, C., Chen, X., Li, X., Li, F., Chen, X., Zou, Y., Wang, W., 2022. Effects of hydrological environment on litter carbon input into the surface soil organic carbon pool in the Dongting Lake floodplain. *Catena* 208, 105761.